

## Spin-Orbit Coupling, Spin Relaxation, and Spin Diffusion in Organic Solids

Z. G. Yu

*Physical Sciences Division, SRI International, 333 Ravenswood Avenue, Menlo Park, California 94025, USA*  
(Received 30 September 2010; published 11 March 2011)

We develop a systematic approach of quantifying spin-orbit coupling (SOC) and a rigorous theory of carrier spin relaxation caused by the SOC in disordered organic solids. The SOC mixes up and down spin in the polaron states and can be characterized by an admixture parameter  $\gamma^2$ . This mixing effects spin flips as polarons hop from one molecule to another. The spin relaxation time is  $\tau_{sf} = \bar{R}^2/(16\gamma^2 D)$ , and the spin diffusion length is  $L_s = \bar{R}/4|\gamma|$ , where  $\bar{R}$  is the mean polaron hopping distance and  $D$  the carrier diffusion constant. The SOC in tris-(8-hydroxyquinoline) aluminum (Alq<sub>3</sub>) is particularly strong due to the orthogonal arrangement of the three ligands. The theory quantitatively explains the temperature-dependent spin diffusion in Alq<sub>3</sub> from recent muon measurements.

DOI: 10.1103/PhysRevLett.106.106602

PACS numbers: 72.80.Le, 71.70.Ej, 72.25.Rb, 76.30.Pk

Spintronics is a rapidly growing field because of its broad applications and fascinating science [1]. Organic spintronics is motivated by weak spin-orbit couplings (SOCs) and hyperfine interactions (HFIs), the two major sources of spin relaxation (SR), of light constituent elements in organic materials [2]. To date, however, there is little quantification of these interactions in individual organic materials, which prevents a meaningful comparison among different organics. In addition, carrier SR in organics, especially that due to the SOC, is poorly understood [3]. The organic solids used in spintronic device structures are usually in the form of dense thin films, which are neither crystalline nor molecules in a solution. Hence, SR theories developed for crystalline inorganic semiconductors, such as the classic works by Elliott and Yafet [4] and by D'yakonov and Perel' [5], are not directly applicable. Nor are the SR theories for isolated organic molecules [6,7], where spins are immobile. Fundamentally, SR of mobile electrons (carriers) should be closely related to carrier transport (e.g., mobility) [4,5], which is via hopping and, frequently, variable-range hopping [8,9] in organic solids [10,11]. In this Letter, we define a SOC measure and calculate its values in various organics. Then we develop a theory of SR caused by the SOC.

In conjugated organic materials, the electronic states are primarily derived from the  $p$  orbitals of carbon in an  $sp^2$ - $p_z$  hybrid configuration, in which the  $sp^2$  orbitals form  $\sigma$  bonds and determine the molecular structure, whereas the  $p_z$  orbitals form  $\pi$  bonds, which are mainly responsible for low-energy electrical and optical processes. In fact, the celebrated Su-Schrieffer-Heeger model [12] contains only  $\pi$  electrons explicitly. However,  $\pi$ -electron models are inherently inadequate to study SOC (and HFI [13]), because by definition, the SOC enables transfer of angular momenta between orbitals and spins. By neglecting the  $\sigma$  ( $p_x$  and  $p_y$ ) electrons, the orbital angular momentum is completely quenched and so is the SOC [15–17]. To see the SOC effect, as a heuristic example,

we consider the case of a molecule in a  $2p$  state subjected to a potential field that lowers the energy of the  $p_z$  orbital relative to  $p_x$  and  $p_y$  by  $\Delta$  (to mimic  $\sigma$ - $\pi$  energy splitting). The SOC of  $2p$  states is  $\lambda \mathbf{l} \cdot \mathbf{s}$ . If the spin quantization axis is along the  $z$  axis, from perturbation, the lowest-energy eigenstate of the systems with spin primarily being up (down) is

$$|+(-)\rangle = |p_z \uparrow (\downarrow)\rangle + (-) \frac{\lambda}{2\Delta} [|p_x + (-)ip_y\rangle \downarrow (\uparrow)\rangle]. \quad (1)$$

These two eigenstates, degenerate in energy (the energy corrections due to the SOC are both  $-\frac{\lambda^2}{2\Delta}$ ), have both up- and down-spin components, rendering spin not a good quantum number. Equation (1) suggests that we can use the percentage of down spin in a predominantly up-spin eigenstate to measure the SOC strength:  $\gamma^2 = \lambda^2/2\Delta^2$ . This measure, which survives any SU(2) rotation in the spin space, depends on not only the SOC ( $\lambda$ ) but also the  $\sigma$ - $\pi$  splitting ( $\Delta$ ), indicating the necessity of explicit inclusion of  $\sigma$  electrons in describing the SOC.

In an organic solid, the molecular (orbital) orientations are randomly distributed, whereas the spin quantization axis is well defined, along either an applied magnetic field or magnetic contacts, which is fixed along the  $z$  axis in this paper. For the molecule oriented along  $(\theta, -\phi)$  in the spherical coordinates, the lowest eigenstate for “up” spin, after taking into account the SOC, is [18]

$$|+\rangle = |p'_z \uparrow\rangle - \frac{i\lambda}{2\Delta} [\sin\theta |p'_y \uparrow\rangle - e^{i\phi} \cos\theta |p'_y \downarrow\rangle + ie^{i\phi} |p'_x \downarrow\rangle], \quad (2)$$

where  $p'_q$  ( $q = x, y, z$ ) is the orbital in the local coordinates. Again the SOC causes a spin mixing of  $\gamma_{\uparrow\downarrow}^2 = \frac{\lambda^2}{4\Delta^2} \times (1 + \cos^2\theta)$ . In addition, it gives rise to an orbital mixing:  $\gamma_{\uparrow\uparrow}^2 = \frac{\lambda^2}{4\Delta^2} \sin^2\theta$ . Since an intrinsic property like SOC should not depend on the molecular orientation, a suitable SOC measure is the combination of the orbital mixing and

spin mixing:  $\gamma^2 = \gamma_{\uparrow\uparrow}^2 + \gamma_{\uparrow\downarrow}^2 = \frac{\lambda^2}{2\Delta^2}$ , which is also the maximum of spin mixing.

For realistic organics, we focus on the highest occupied molecular orbitals (HOMOs) of a negatively charged and positively charged molecule or oligomer, which corresponds to the electron and hole polarons. The total Hamiltonian of an organic molecule can be written as

$$H = H_0 + H_{SO} = H_0 + \sum_i \xi_i l_i \cdot s_i, \quad (3)$$

where  $H_{SO}$  is the summation of all atomic SOC contributions. The SOC is nonzero for  $p$  orbitals, and the coupling strengths are  $\xi = 28, 76$ , and  $151 \text{ cm}^{-1}$  for  $2p$  orbitals in C, N, and O, respectively, and  $382$  and  $112 \text{ cm}^{-1}$  for  $3p$  orbitals in S and Al, respectively [19]. Because of these weak SOC's compared to bonding energies, in most first-principles calculations of organic materials the SOC is completely ignored; i.e., the obtained eigenstates  $|\psi_k\rangle$  are those of  $H = H_0$ , which are our starting point and can be expanded in terms of the atomic orbitals:

$$|\psi_k\rangle = \sum_{i\alpha} c_{i\alpha}^{(k)} |\phi_i^{(\alpha)}\rangle,$$

where  $k$  is the index of eigenstates.  $|\phi_i^{(\alpha)}\rangle$  is the  $\alpha$ th atomic orbital at the  $i$ th molecule, and  $\phi^{(\alpha)} = 2s, 2p_x, 2p_y, 2p_z$  for O, N, and C,  $\phi^{(\alpha)} = 1s$  for H, and  $\phi^{(\alpha)} = 3s, 3p_x, 3p_y, 3p_z$  for S and Al. Since the atomic orbitals are not orthogonal, the normalization condition is  $\sum_{i\alpha} \sum_{j\alpha'} c_{i\alpha}^{(k)} c_{j\alpha'}^{(k)} S_{ij}^{(\alpha\alpha')} = \delta_{kk'}$ , where  $S_{ij}^{(\alpha\alpha')} = \langle \phi_i^{(\alpha)} | \phi_j^{(\alpha')} \rangle$ . For the HOMO  $|\psi_0\rangle$ , the eigenstate of the up spin after taking into account  $H_{SO}$  is

$$|\psi_0, +\rangle = |\psi_0, \uparrow\rangle - \frac{1}{2} \sum_{k \neq 0} \frac{\langle \psi_k | \sum_i \xi_i l_{iz} | \psi_0 \rangle}{E_k - E_0} |\psi_k, \uparrow\rangle \\ - \frac{1}{2} \sum_{k \neq 0} \frac{\langle \psi_k | \sum_i \xi_i (l_{ix} + il_{iy}) | \psi_0 \rangle}{E_k - E_0} |\psi_k, \downarrow\rangle,$$

where  $k$  runs over all possible eigenstates of  $H_0$  and  $l_{iq}$  is the  $q$  component angular momentum at atom  $i$ . Using  $l_{iq} p_r = i\epsilon_{qrs} p_s$  for  $p$  orbitals at atom  $i$  with  $\epsilon_{qrs}$  being the unit axial tensor, we express  $|\psi_0, +\rangle$  as

$$|\psi_0, +\rangle = |\psi_0, \uparrow\rangle + \sum_{i\alpha} (a_{i\alpha} |\phi_i^{(\alpha)} \uparrow\rangle + b_{i\alpha} |\phi_i^{(\alpha)} \downarrow\rangle). \quad (4)$$

The admixture parameter that measures the SOC is

$$\gamma^2 = \gamma_{\uparrow\uparrow}^2 + \gamma_{\uparrow\downarrow}^2 \equiv \sum_{ij} (a_{i\alpha}^* a_{j\alpha'} + b_{i\alpha}^* b_{j\alpha'}) S_{ij}^{(\alpha\alpha')}. \quad (5)$$

We calculate  $\gamma^2$  by using  $|\psi_k\rangle$  of the optimized molecular geometry obtained from SIESTA [20] and list its values for representative organic materials in Table I. Surprisingly, the SOC in tris-(8-hydroxyquinoline) aluminum ( $\text{Alq}_3$ ) is stronger by orders of magnitude than in phenylenevinylene and rubrene and even much stronger than  $T_6$ , where S has a larger atomic SOC than N, O, and

TABLE I. Spin-orbit coupling measure  $|\gamma|$ .

Material	Electron polaron	Hole polaron
$\text{Alq}_3$	$2.75 \times 10^{-2}$	$6.91 \times 10^{-3}$
Sexithiophene ( $T_6$ )	$4.09 \times 10^{-3}$	$2.57 \times 10^{-3}$
Phenylenevinylene	$4.04 \times 10^{-4}$	$2.55 \times 10^{-3}$
Rubrene	$2.97 \times 10^{-4}$	$3.25 \times 10^{-4}$
Benzene	$2.75 \times 10^{-4}$	$3.06 \times 10^{-4}$

Al in  $\text{Alq}_3$ . Having examined individual terms in Eq. (4), we find that the strong SOC in  $\text{Alq}_3$  is due mainly to the orthogonal arrangement of the three conjugated ligands. To corroborate this conclusion we study the SOC in a biphenyl molecule, which contains only C and H atoms, as a function of the torsion angle  $\theta$  between the two rings. We see in Fig. 1 a strong dependence of  $\gamma^2$  on the torsion, especially near  $\theta = \pi/2$ , where the  $\pi$  orbitals in the two rings are perpendicular to each other and degenerate in energy, as shown in the inset in Fig. 1. Since in organic solids the molecules or oligomers may be packed differently from sample to sample, the torsion dependence shown in Fig. 1 suggests that the SOC in organics can be influenced by how the material is prepared.

Now we show that the SOC-induced spin mixing in polaron states can cause SR as polaron hops. Consider two molecules with orientations  $(\theta_i, \phi_i)$  and  $(\theta_j, \phi_j)$ . The electron-phonon interaction  $V$ , which facilitates polaron hopping, does not depend on spin and cannot flip spin by itself:  $\langle p'_q \uparrow | V | p'_r \downarrow \rangle = 0$ , where  $p'_q$  ( $p'_q$ ) represents orbitals of molecule  $i$  ( $j$ ) in local coordinates. However, owing to the spin mixing, the matrix element from the eigenstate for up spin  $|+\rangle$  in molecule  $i$  to that for “down” spin  $|-\rangle$  in molecule  $j$  is finite:

$$\langle -'' | V | +' \rangle = \frac{\lambda}{2\Delta} [i \cos\theta_1 e^{-i\phi_1} V_{z''y'} - i \cos\theta_2 e^{-i\phi_2} V_{y''z'} \\ + e^{-i\phi_1} V_{z''x'} - e^{-i\phi_2} V_{x''z'}], \quad (6)$$

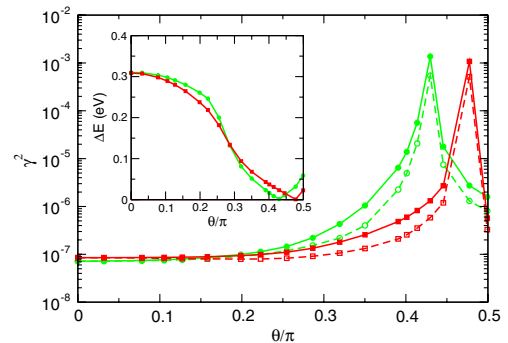


FIG. 1 (color online). Admixture  $\gamma^2$  as a function of torsion angle  $\theta$  in biphenyl. Green (light gray) and red (dark gray) lines are for the electron and hole polarons, respectively. Solid (dashed) lines describe  $\gamma^2$  ( $\gamma_{\uparrow\uparrow}^2$ ). The inset shows the energy splitting between the HOMO and HOMO + (-)1 for the electron (hole) polaron.

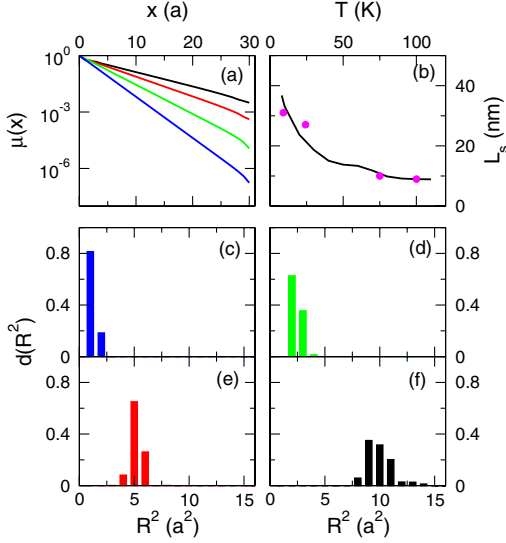


FIG. 2 (color online). (a) Logarithm of spin polarization as a function of  $x$  with spin injected at the plane of  $x = 0$  in a  $32 \times 32 \times 32$  cubic lattice by numerically solving Eq. (11). The four lines, from bottom to top, correspond to  $T = 80, 40, 20,$  and  $10$  K, respectively. (b) Spin diffusion length as a function of temperature for  $\text{Alq}_3$ . Circles are experimental values. (c)–(f) are the distributions of hopping distance at  $T = 80, 40, 20,$  and  $10$  K, respectively.

where  $V_{q''r'} = \langle p'' \uparrow | V | p' \uparrow \rangle$  is spin-independent and

$$V_{q''r'}(\theta_i, \phi_i; \theta_j, \phi_j) = \sum_{lm} O_{ql}^{-1}(\theta_j, \phi_j) V_{l'm'}(0) O_{mr}(\theta_i, \phi_i),$$

where  $O(\theta, \phi)$  is the  $\text{SO}(3)$  rotation matrix and  $V_{l'm'}(0)$  represents the matrix element for  $(\theta_i, \phi_i) = (\theta_j, \phi_j) = (0, 0)$ . Without losing generality, we assume  $|V_{x''x'}(0)| = |V_{y''y'}(0)| = |V_{z''z'}(0)| = v_0$  between parallel orbitals and  $|V_{x''y'}(0)| = |V_{y''z'}(0)| = |V_{x''z'}(0)| = v_1$  between perpendicular orbitals. After averaging over  $(\theta_i, \phi_i)$  and  $(\theta_j, \phi_j)$ , we have  $|\langle -'' | V | +'' \rangle|^2 = \frac{(\Delta)^2}{9} (v_0^2 + 2v_1^2)$ , and for spin-conserving hopping,  $|\langle +'' | V | +'' \rangle|^2 = \frac{1}{3}(v_0^2 + 2v_1^2)$ . Thus each polaron hop contains both spin-conserving and spin-flip contributions (their hopping rates are  $w^{++}$  and  $w^{-+}$ ), and the percentage of the spin-flip hopping is

$$\chi^2 = \frac{w^{-+}}{w^{++}} = \frac{|\langle -'' | V | +'' \rangle|^2}{|\langle +'' | V | +'' \rangle|^2} = \frac{4}{3} \gamma^2. \quad (7)$$

We emphasize that  $|\langle -'' | V | +'' \rangle|^2$  and therefore  $w^{-+}$  are invariant under any  $\text{SU}(2)$  rotation. The spin-conserving hopping rate is directly related to the carrier diffusion constant  $D = \frac{1}{6} w^{++} \bar{R}^2$  [21]. The SR rate, which can be measured by pulsed electrically detected magnetic resonance [22], is [6]

$$\tau_{\text{sf}}^{-1} = w^{-+} + w^{+-} = 2w^{-+} = 16\gamma^2 D / \bar{R}^2. \quad (8)$$

Equation (8) indicates that the SOC-induced SR increases with the carrier diffusion constant, and the SR time

becomes longer at lower temperatures, where the polaron hopping is less frequent. The spin diffusion (SD) length, which can be directly measured by muon spin resonance [23] and two-photo photoemission [24], is

$$L_s \equiv \sqrt{D\tau_{\text{sf}}} = \frac{\bar{R}}{4\gamma}. \quad (9)$$

This remarkably simple expression shows that the SD length is essentially controlled by the admixture parameter, and by improving the mobility the SD length will not be enhanced. Based on the SOC values in Table I and Eqs. (8) and (9),  $\tau_{\text{sf}}$  and  $L_s$  can vary significantly from one organic solid to another, in the range  $10^{-6}$ – $10^{-2}$  s and 10–1000 nm, respectively.

The SR and SD can be more rigorously discussed by using the density-matrix theory. The polaron hopping can be written as  $\hat{V} = \sum_{ij} \hat{V}_{ij}$ , where the matrix elements between polaron eigenstates in molecules  $i$  and  $j$  is  $\hat{V}_{ji} = V_{ji}^0 \hat{1} + \sum_q \hat{\sigma}_q V_{ji}^q$ , where  $\hat{\sigma}_q$  are the Pauli matrices.  $V_{ji}^0 = (\langle +'' | V | +'' \rangle + \langle -'' | V | -'' \rangle) / 2 = V_{p''_j p''_i}$ ,  $V_{ji}^x = (\langle -'' | V | +'' \rangle + \langle +'' | V | -'' \rangle) / 2$ ,  $V_{ji}^y = (\langle -'' | V | +'' \rangle - \langle +'' | V | -'' \rangle) / 2i$ , and  $V_{ji}^z = (\langle +'' | V | +'' \rangle - \langle -'' | V | -'' \rangle) / 2$ . The spin-polarized carrier density is  $\hat{\rho} = \sum_i \hat{\rho}_i$  with  $\hat{\rho}_i = \rho_i^0 \hat{1} + \sum_q \hat{\sigma}_q \rho_i^q$ , where  $\rho_i^0$  is the equilibrium up- or down-spin carrier density in the absence of spin polarization. The density matrix obeys the following Redfield equation in the interaction representation [6]:

$$\frac{d\hat{\rho}}{dt} = -\frac{i}{\hbar} [\hat{V}(t), \hat{\rho}(0)] - \frac{1}{\hbar^2} \times \int_0^\infty d\tau \overline{[\hat{V}(t), [\hat{V}(t-\tau), \hat{\rho}(0)]]},$$

which, after projecting  $\hat{\rho}$  into site  $i$  and spin component  $q$ , becomes

$$\frac{d\rho_i^q}{dt} = -\frac{1}{\hbar^2} \sum_j \left[ \rho_j^q L_{ij}^0(\omega_{ij}) \left( 1 + \chi_q^2 + \sum_{r \neq q} \chi_r^2 \right) - \rho_j^q L_{ji}^0(\omega_{ji}) \left( 1 + \chi_q^2 - \sum_{r \neq q} \chi_r^2 \right) \right], \quad (10)$$

where  $L_{ij}^0$  is the temporal correlation function

$$L_{ij}^0(\omega) = \int_{-\infty}^{+\infty} \overline{V_{ij}^0(t) V_{ji}^0(t+\tau)} e^{-i\omega\tau} d\tau$$

and  $\omega_{ij} = (E_i - E_j) / \hbar$  with  $E_i$  being the polaron energy at molecule  $i$ . Here we have used  $\int_{-\infty}^{+\infty} \overline{V_{ij}^q(t) V_{ji}^q(t+\tau)} e^{-i\omega\tau} = \delta_{qq'} L_{ij}^0(\omega) \chi_q^2$ . It is readily proven that  $\chi_x^2 = \chi_y^2 = \chi_z^2 = \chi^2 / 2$  for random molecular orientations. To describe carrier spins in disordered organic solids, it is advantageous to use a spin-polarized electrochemical potential  $\hat{\mu}_i = \mu_i^0 \hat{1} + \sum_q \hat{\sigma}_q \mu_i^q$ , which is related to the local density polarization as  $\rho_i^q = \rho_i^0 \mu_i^q / k_B T$  in the nondegenerate systems with  $k_B$  being the Boltzmann constant

and  $T$  temperature [25]. Noticing  $\frac{1}{\hbar^2}L_{ij}^0(\omega_{ij})(1 + \chi_q^2) \simeq \frac{1}{\hbar^2}L_{ij}^0(\omega_{ij}) = w_{ij} \equiv w_{ij}^{+}$  [6,7] and  $\rho_i^0 w_{ij} = \rho_j^0 w_{ji}$ , we rewrite Eq. (10) as

$$\frac{\rho_i^0}{k_B T} \frac{d\mu_i^q}{dt} = \sum_j Z_{ij}^{-1} [(1 - \chi^2)\mu_j^q - (1 + \chi^2)\mu_i^q], \quad (11)$$

where  $Z_{ij}^{-1} = \rho_i^0 w_{ij}/k_B T = \rho_j^0 w_{ji}/k_B T$ .

To determine the carrier SR time, we track the time evolution of a spatially homogeneous spin polarization  $\mu^q$ , and, in this case, Eq. (11) reads

$$d\mu^q/dt = -2\chi^2 \mu^q k_B T \sum_{ij} Z_{ij}^{-1} / \sum_i \rho_i^0 \equiv -\mu^q / \tau_{sf}. \quad (12)$$

Thus  $\tau_{sf}^{-1} = (8\gamma^2/3)k_B T \sum_{ij} Z_{ij}^{-1} / \sum_i \rho_i^0$ , which is identical to Eq. (8) if we employ the Kubo formula for the diffusion constant in disordered systems,  $D = \sum_i \rho_i^0 w_{ij} R_{ij}^2 / 6 \sum_i \rho_i^0$ , where  $R_{ij} = |\mathbf{R}_{ij}|$  and  $\mathbf{R}_{ij}$  is the displacement between molecules  $i$  and  $j$ , and define  $\bar{R}$  as  $\bar{R}^2 = \sum_{ij} Z_{ij}^{-1} R_{ij}^2 / \sum_{ij} Z_{ij}^{-1}$  (the meaning of  $\bar{R}$  used before is clarified). To determine the SD length, we examine the spatial dependence of spin polarization in a steady state ( $d\mu^q/dt = 0$ ). By expanding  $\mu^q(\mathbf{r}_j) = \mu^q(\mathbf{r}_i) + \mathbf{R}_{ji} \cdot \nabla \mu^q(\mathbf{r}_i) + \frac{1}{2} \mathbf{R}_{ji} \mathbf{R}_{ji} : \nabla \nabla \mu^q(\mathbf{r}_i)$  and summing over  $i$ , Eq. (11) is reduced to

$$\sum_{ij} Z_{ij}^{-1} \left[ -2\chi^2 \mu^q(\mathbf{r}_i) + \frac{1}{6} R_{ij}^2 \nabla^2 \mu^q(\mathbf{r}_i) \right] = 0. \quad (13)$$

Comparing it to the definition of SD length  $L_s$ ,  $(\nabla^2 - L_s^{-2})\mu^q(\mathbf{r}) = 0$ , we find  $L_s = \bar{R}/4\gamma$ , as in Eq. (9).

To reveal microscopic details of SD and to directly model the muon experiments in  $\text{Alq}_3$ , we solve Eq. (11) in a  $32 \times 32 \times 32$  cubic lattice with one plane ( $x = 0$ ) assigned a constant  $\mu^q = 1$  and the opposite plane ( $x = 31a$ )  $\mu^q = 0$ . The lattice constant  $a$  is set 13 Å, slightly larger than the diameter of an  $\text{Alq}_3$  molecule, 11.4 Å. In the lattice polarons can hop between any two sites, and therefore the variable-range hopping [8,9] is automatically included in the model. The hopping probability is assumed to have the Efros-Shklovskii form [9]:  $w_{ij} = w_0 e^{-2R_{ij}/\ell} e^{(E_i - E_j - e^2/\varepsilon R_{ij})/k_B T}$ , where  $\ell$  is the polaron delocalization length and  $e^2/\varepsilon R_{ij}$  is the Coulomb interaction between the created electron-hole pair after a polaron hop with  $\varepsilon$  being the dielectric constant. We plot  $\mu(x)$ , the averaged  $\mu_i^q$  over the  $y$ - $z$  plane for a given  $x$ , in Fig. 2(a), which is seen to decay exponentially over distance:  $\mu(x) \sim e^{-x/L_s}$ . The parameters are  $\ell = 0.6 \text{ \AA}^{-1}$ ,  $|\gamma| = 0.1375$ , and  $e^2/\varepsilon a = 0.3 \text{ eV}$ ,  $\gg |E_i - E_j|$ . Here we artificially increase  $|\gamma|$  by 5 times to ensure a converging SD length within the cubic lattice. We multiply the obtained SD lengths from Fig. 2(a) by 5 and plot them in Fig. 2(b). The agreement between the experiment and theory is excellent. The SD length saturates at high temperatures and increases as temperature lowers. From the distribution of polaron hopping distances  $d(R^2) \equiv \sum_{ij} Z_{ij}^{-1} (R_{ij}^2 = R^2) / \sum_{ij} Z_{ij}^{-1}$ , shown in Figs. 2(c)–2(f),

we see that the increase in  $L_s$  at low temperatures is due to the enhanced polaron hopping distance  $\bar{R}$  and that the saturation occurs because polaron hoppings are confined to nearest neighbors ( $\bar{R} = a$ ) above 80 K.

The HFI can also cause carrier SR with a rate of  $\tau_H^{-1} \propto H_f^2 \tau_d$  [26,27], where  $H_f^2$  is the HFI field variance and  $\tau_d$  is the polaron dwell time at one molecule:  $\tau_d \propto 1/D$ . Thus both the SR time  $\tau_H$  and SD length  $\sqrt{D\tau_H}$  would be linear with  $D$  and rapidly increase with temperature. The disparate temperature dependences between SOC- and HFI-induced SR allow an experimental determination of carrier SR mechanisms in individual organic solids. The agreement displayed in Fig. 2 suggests that carrier SR in  $\text{Alq}_3$  is due mainly to the SOC.

The author is grateful to D.L. Smith for useful discussions. This work was partly supported by the Office of Basic Energy Sciences, Department of Energy, under Grant No. DE-FG02-06ER46325.

- 
- [1] A. Fert, *Rev. Mod. Phys.* **80**, 1517 (2008).
  - [2] Editorial, *Nature Mater.* **8**, 691 (2009).
  - [3] G. Szulczewski *et al.*, *Nature Mater.* **8**, 693 (2009).
  - [4] Y. Yafet, *Solid State Phys.* **14**, 1 (1963).
  - [5] M. I. D'yakonov and V. I. Perel', *Sov. Phys. JETP* **33**, 1053 (1971).
  - [6] C.P. Slichter, *Principles of Magnetic Resonance* (Springer-Verlag, Berlin, 1978), 2nd ed.
  - [7] Z. G. Yu, *Phys. Rev. B* **77**, 205439 (2008).
  - [8] N. F. Mott, *Adv. Phys.* **16**, 49 (1967).
  - [9] A. L. Efros and B. I. Shklovskii, *J. Phys. C* **8**, L49 (1975).
  - [10] J. H. Shim *et al.*, *Phys. Rev. Lett.* **100**, 226603 (2008).
  - [11] Z. G. Yu and X. Song, *Phys. Rev. Lett.* **86**, 6018 (2001).
  - [12] W. P. Su, J. R. Schrieffer, and A. J. Heeger, *Phys. Rev. B* **22**, 2099 (1980).
  - [13]  $\pi$  orbitals give zero electron density at both carbon atoms and nearby hydrogen atoms and would lead to zero isotropic HFI if  $\sigma$  orbitals were not included [14].
  - [14] H. M. McConnell, *J. Chem. Phys.* **24**, 764 (1956).
  - [15] D. S. McClure, *J. Chem. Phys.* **20**, 682 (1952).
  - [16] J. Rybicki and M. Wohlgenannt, *Phys. Rev. B* **79**, 153202 (2009); J. Rybicki *et al.*, *Synth. Met.* **160**, 280 (2010).
  - [17] By neglecting  $p_x$  and  $p_y$ ,  $l_q |p_z\rangle = l^2 |p_z\rangle = 0$  ( $q = x, y, z$ ).
  - [18]  $|+\rangle$  has the largest spin expectation value along the  $z$  axis:  $\langle + | \sigma_z | + \rangle = 1 - \lambda^2 \cos^2 \theta / 2\Delta^2$ .
  - [19] See, e.g., <http://www.nist.gov/physlab/data/asd.cfm>.
  - [20] J. M. Soler *et al.*, *J. Phys. Condens. Matter* **14**, 2745 (2002).
  - [21] D. Emin, *Adv. Phys.* **24**, 305 (1975).
  - [22] D. R. McCamey *et al.*, *Nature Mater.* **7**, 723 (2008).
  - [23] A. J. Drew *et al.*, *Nature Mater.* **8**, 109 (2009).
  - [24] M. Cinchetti *et al.*, *Nature Mater.* **8**, 115 (2009).
  - [25] Z. G. Yu, M. A. Berding, and S. Krishnamurthy, *Phys. Rev. B* **71**, 060408(R) (2005).
  - [26] M. I. D'yakonov and V. I. Perel', *Sov. Phys. JETP* **38**, 177 (1974).
  - [27] P. A. Bobbert *et al.*, *Phys. Rev. Lett.* **102**, 156604 (2009).